

Two-dimensional PC_3 as a promising anode material for potassium-ion batteries: First-principles calculations

Chun Zhou(周淳), Junchao Huang(黄俊超), Xiangmei Duan(段香梅)

Citation: Chin. Phys. B, 2021, 30 (**5**): 056801. DOI: 10.1088/1674-1056/abf10e
Journal homepage: http://cpb.iphy.ac.cn; http://iopscience.iop.org/cpb

What follows is a list of articles you may be interested in

Selective linear etching of monolayer black phosphorus using electron beams

Yuhao Pan(潘宇浩), Bao Lei(雷宝), Jingsi Qiao(乔婧思), Zhixin Hu(胡智鑫), Wu Zhou(周武), Wei Ji(季威)
Chin. Phys. B, 2020, 29 (**8**): 086801. DOI: 10.1088/1674-1056/ab9438

High quality $PdTe_2$ thin films grown by molecular beam epitaxy

En Li(李恩), Rui-Zi Zhang(张瑞梓), Hang Li(李航), Chen Liu(刘晨), Geng Li(李更), Jia-Ou Wang(王嘉鸥), Tian Qian(钱天), Hong Ding(丁洪), Yu-Yang Zhang(张余洋), Shi-Xuan Du(杜世萱), Xiao Lin(林晓), Hong-Jun Gao(高鸿钧)
Chin. Phys. B, 2018, 27 (**8**): 086804. DOI: 10.1088/1674-1056/27/8/086804

Direct measurements of conductivity and mobility in millimeter-sized single-crystalline graphene via van der Pauw geometry

Rui-Song Ma(马瑞松), Qing Huan(郇庆), Liang-Mei Wu(吴良妹), Jia-Hao Yan(严佳浩), Yu-Yang Zhang(张余洋), Li-Hong Bao(鲍丽宏), Yun-Qi Liu(刘云圻), Shi-Xuan Du(杜世萱), Hong-Jun Gao(高鸿钧)
Chin. Phys. B, 2017, 26 (**6**): 066801. DOI: 10.1088/1674-1056/26/6/066801

Geometric stability and electronic structure of infinite and finite phosphorus atomic chains

Jingsi Qiao(乔婧思), Linwei Zhou(周霖蔚), Wei Ji(季威)
Chin. Phys. B, 2017, 26 (**3**): 036803. DOI: 10.1088/1674-1056/26/3/036803

Photodetecting and light-emitting devices based on two-dimensional materials

Yuanfang Yu(于远方), Feng Miao(缪峰), Jun He(何军), Zhenhua Ni(倪振华)
Chin. Phys. B, 2017, 26 (**3**): 036801. DOI: 10.1088/1674-1056/26/3/036801

Two-dimensional PC_3 as a promising anode material for potassium-ion batteries: First–principles calculations*

Chun Zhou(周淳), Junchao Huang(黄俊超), and Xiangmei Duan(段香梅)†

School of Physical Science and Technology, Ningbo University, Ningbo 315211, *China*

(Received 6 January 2021; revised manuscript received 3 March 2021; accepted manuscript online 23 March 2021)

With the diversified development of the battery industry, potassium-ion batteries (PIBs) have aroused widespread interest due to their safety and high potassium reserves on earth. However, the lack of suitable anode materials limits their development and application to a certain extent. Based on first-principles calculations, we investigate the possibility of using PC_3 monolayer as the anode material for PIBs. PC_3 sheet has excellent electrical properties and meets the prerequisite of anode materials. The storage capacity of potassium is as high as 1200 mAh·g^{-1}, which is better than many other reported potassium-ion anode materials. In addition, the outstanding advantages of PC_3 sheet, such as low diffusion barrier and moderate open-circuit voltage, make it a potential anode candidate for PIBs.

Keywords: two-dimensional materials, potassium-ion batteries, first-principles

PACS: 68.65.−k, 82.47.Cb, 71.20.Nr, 71.15.Mb **DOI:** 10.1088/1674-1056/abf10e

1. Introduction

In recent years, with the rapid development of the electronic market, the demand for innovative batteries with excellent performance has been increasing. So far, lithium-ion batteries (LIBs) are the most widely used batteries, with high power density, great charge–discharge efficiency, and long life cycle. However, the lithium resources on the earth are limited and its stocks are falling, which poses a challenge to the development of LIBs. With the growing interest in LIBs alternatives, it is urgent to find suitable new electrode materials.[1] Since the outer electronic structure and electrical properties are similar to LIBs, sodium-ion batteries (SIBs) and potassium-ion batteries (PIBs) have been proposed to resolve this crisis. Compared with LIBs, they have the advantages of low cost, high safety, and abundant reserves on the earth. Meanwhile, the mature theoretical knowledge and technical experience of LIBs can be applied to SIBs and PIBs to a certain extent. Compared with SIBs, LIBs have higher voltage and energy density due to lower standard electrode potential. However, the standard electrode potential of K^+/K is comparable to, or even lower than, that of Li^+/Li, which indicates that PIBs have higher voltage and energy density.[2] Taking these factors into consideration, we regard PIBs as a more appropriate choice. However, the lack of suitable anode materials hindered the development of PIBs.

Since the successful exfoliation of graphene in 2004, two-dimensional (2D) materials have received widespread attention due to their excellent physical and chemical properties. As anode materials of ion batteries, 2D materials have also shown outstanding performance. For instance, graphene nanosheet families exhibit excellent behavior in rechargeable LIBs.[3] Phosphorene has attracted much attention due to its remarkably high theoretical capacity (2596 mAh·g^{-1}) in SIBs.[4] Phosphorene and graphene heterostructure have also been investigated as the anode for LIBs.[5] However, these materials are not suitable for PIBs, partly because potassium has a larger atomic radius. Several 2D materials have been proposed as anode for PIBs, such as $FeSe_2$,[6] GeSe,[7] YN_2,[8] and T-$NiSe_2$.[9] However, as an emerging novel ion battery, PIBs choice is far from enough. Therefore, it is necessary to explore high-performance anode materials for PIBs.

It has been reported that metallic P_3C and PC_3 monolayer can be used as anode for SIBs, and 2D PC_6 sheet is a promising anode material for PIBs.[10–12] Due to the excellent conductivity and stability of the material composed of C elements and the high specific capacity of P-based materials, we focus on the 2D binary materials of P and C. Similarly, 2D binary materials g-SiC_2 and g-SiC_3 have been used as anode materials for LIBs. And they have shown excellent performance by combining the good qualities of both elements Si and C.[13] After a series of screening and testing, we finally choose the PC_3 monolayer, which is a stable hexagonal structure similar to graphene, with high theoretical capacity and low voltage, and is very suitable to be anode material for PIBs.

2. Computational method

All calculations are performed using density functional theory (DFT) as implemented in the Vienna *ab initio* simulation package (VASP).[14,15] The Perdew–Burke–Ernzerhof

*Project supported by the National Natural Science Foundation of China (Grant Nos. 11574167 and 11874033) and the KC Wong Magna Foundation in Ningbo University.

†Corresponding author. E-mail: duanxiangmei@nbu.edu.cn

© 2021 Chinese Physical Society and IOP Publishing Ltd

(PBE) functional of the generalized gradient approximation (GGA) is used to describe the exchange–correlation interactions.[16] The Brillouin zones are sampled using a $3\times3\times1$ k-point grid according to the Monkhorste–Pack scheme for a 2×2 supercell.[17] The kinetic energy cutoff of 700 eV is used for all calculations. To avoid periodic image interactions, a vacuum space of 20 Å is set along the z direction to the PC_3 monolayer. The projector augmented wave (PAW) method is adopted to describe interactions among ion cores and valence electrons.[18] The DFT-D3 method for van der Waals interaction description is adopted.[19] All the structures are thoroughly relaxed until the forces are less than 10^{-2} eV/Å, and the energy convergence is below 10^{-5} eV between two consecutive self-consistent steps. The migration pathways and diffusion barriers for K atoms on the PC_3 monolayer are calculated using the climbing image nudged elastic band (CI-NEB) method. To verify the stability of PC_3 monolayer, *ab initio* molecular dynamics (AIMD) simulations using a statistical ensemble with a fixed particle number, volume, and temperature (NVT) are performed at room temperature (300 K) for 5 ps with a time step of 1 fs.

3. Results and discussion

3.1. Structure and stability of PC_3

A rationally designed 2D material PC_3 has a graphene–like hexagonal structure, and each unit cell contains six carbon atoms and two phosphorus atoms. It can be seen from the side view in Fig. 1(a), adjacent phosphorus atoms are distributed on different sides, making PC_3 a buckled material with an up–and–down thickness of 1.19 Å. The optimized lattice parameters of the PC_3 monolayer are $a=b=5.42$ Å, $\alpha=\beta=90^\circ$ and $\gamma=120^\circ$. The average C–C bond length is 1.42 Å, the same as in graphene, and the average P–C bond length is 1.81 Å, comparable to the values of 1.80–1.83 Å in phosphorus carbide.[20]

To verify PC_3 monolayer can be synthesized experimentally, we calculate its cohesive energy, $E_{\rm coh}$, which is defined as

$$E_{\rm coh}=(6E_{\rm C}+2E_{\rm P}-E_{\rm PC_3})/8, \tag{1}$$

where $E_{\rm C}$, $E_{\rm P}$, and $E_{\rm CP_3}$ are the energy of the isolated C atom, P atom, and PC_3 unit cell, respectively. The value of the cohesive energy is 6.41 eV, which is much higher than that of phosphorene (3.45 eV) and closer to that of graphene (7.98 eV). Such a high cohesive energy indicates that the structure of PC_3 is stable and could be synthesized. We use AIMD simulation to study the thermal stability of the PC_3 monolayer at room temperature. And after 5 ps, no structural deformation or bond fracture occurs, proving its high thermal stability [see Fig. 1(b)].

Now, we calculate the electron local density along the plane of monolayer PC_3 to find the essence of its chemical bonding by using the electron localization function.[21] In Fig. 1(c), the red region between C–C and C–P represents the strong covalent bond. Consistently, the Bader charge analysis shows that each P atom transferred 1.5 $|e|$ to the bonded C atoms, which is attributed to the fact that the electronegativity of C (2.55) is larger than that of P (2.19). It can be seen from Fig. 1(d), PC_3 is an indirect band gap semiconductor (the gap is 0.75 eV). The valence band maximum is located at the M point, and the conduction band minimum is at the Γ point.

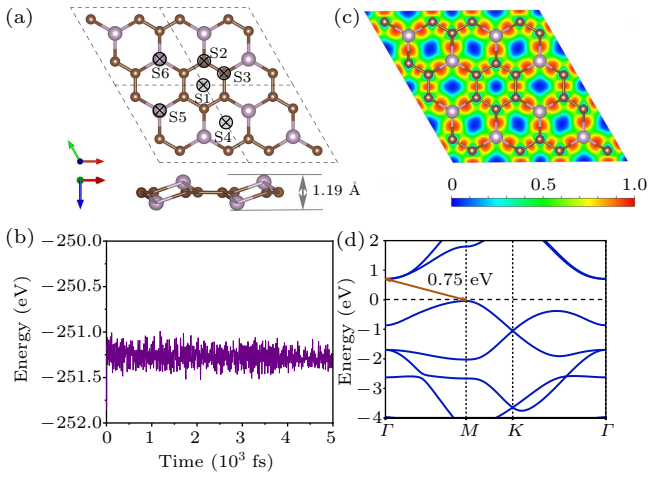


Fig. 1. (a) The top and side view of optimized atomic configurations for PC_3 and different adsorption sites for K ions. (b) The AIMD simulation of PC_3 at 300 K for 5 ps. (c) Localization charge density and (d) band structure of PC_3 monolayer.

3.2. Adsorption and diffusion of K atoms on PC_3

The preference for K adsorption is characterized by the adsorption energy, $E_{\rm ad}$. The lower the energy, the more stable the adsorption configuration. For the K atom on PC_3 monolayer, there are six possible adsorption sites, as marked in Fig. 1(a). The adsorption energy is defined as

$$E_{\rm ad}=E_{\rm K@PC_3}-E_{\rm PC_3}-E_{\rm K}, \tag{2}$$

where $E_{\rm K@PC_3}$ and $E_{\rm PC_3}$ are the total energy of the K-adsorbed and pristine PC_3 monolayers, respectively. And $E_{\rm K}$ is the energy per atom in bulk K. After the optimization, S1, above the center of the C6 ring, has the largest $E_{\rm ad}$ of -0.83 eV. The second stable site is S6, which is on the top of the hollow P atom, with an adsorption energy of -0.79 eV. In contrast to S6, S5 is on the top of the protruding P atom, $E_{\rm ad}$ is -0.74 eV. The vertical distances between the K atom and the PC_3 plane are 2.54 Å, 2.66 Å, and 2.53 Å at S1, S5, and S6 sites. We then focus on the most stable site S1 to study the electrical properties and diffusion barriers.

The charge density difference of K adsorbed PC_3 is shown in Fig. 2(a), where charge accumulates on the surface of PC_3, while charge deletion is around the K atom, indicating

that the charge is transferred from the K atom to PC_3. The charge transferring can be understood by the fact that the electronegativity of C (2.55) is significantly larger than that of K (0.82). The Bader charge analysis manifests that 0.87 $|e|$ transfers from the K atom to the substrate. For other K atoms adsorbed on S5 and S6 sites, the transferred electron is 0.88 $|e|$. Upon potassium adsorption, the system becomes metallic, and the density of states (DOS) is shown in Fig. 2(b). The DOS at the Fermi level is greatly enhanced, and the contribution mainly comes from the substrate PC_3, suggesting that more carriers are generated in the system. Therefore, the electronic conduction becomes better, which is beneficial for PIBs.

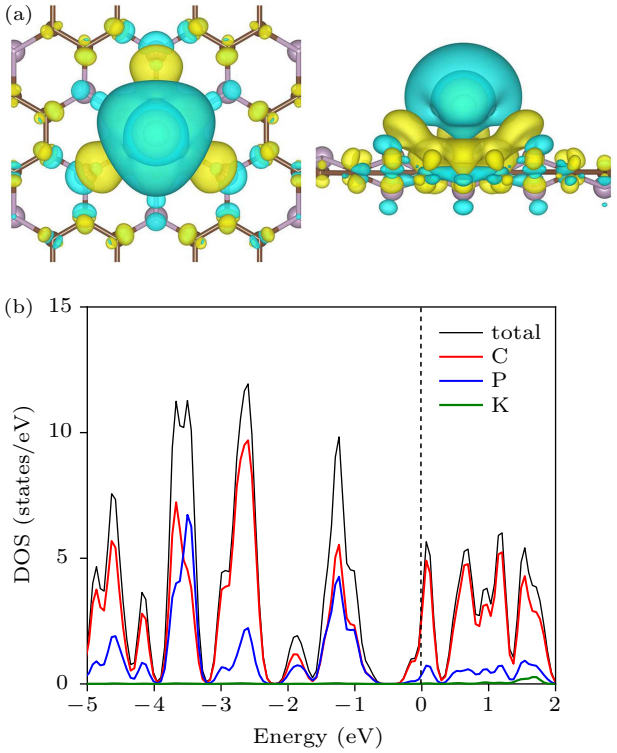


Fig. 2. (a) Charge density difference and (b) band structure of the K-adsorbed PC_3. The yellow and blue regions represent charge accumulation and depletion, respectively. The isosurface level is set to 0.005 $e\cdot$Å^{-3}.

The diffusion rate is a critical parameter for ion batteries. It is partly determined by the adsorption energy between the K atoms and the substrate. On the other hand, the diffusion rate of K atoms on the surface of the anode affects the performance and efficiency of the charging/discharging process to a great extent. To obtain the diffusion energy barrier of the potassium, we consider two possible diffusion pathways for the K atom (denoted as path I and path II) on PC_3, as shown in Fig. 3(a). Via path I, the potassium goes from site S1 to the neighboring S1 directly, across the P_2C_4 ring. Along path II, K moves zigzag from S1 to S6, then to the adjacent S1. The energy barriers via path I and path II are 0.92 eV and 0.16 eV, respectively. Note the energy barrier of 0.16 eV is significantly smaller than the Li diffusion barriers for pristine graphene ($\sim$0.28 eV), graphene with a point defect ($\sim$ 0.366 eV to 0.538 eV),[22] and graphite ($\sim$ 0.47 eV),[23] promising a fast K diffusion.

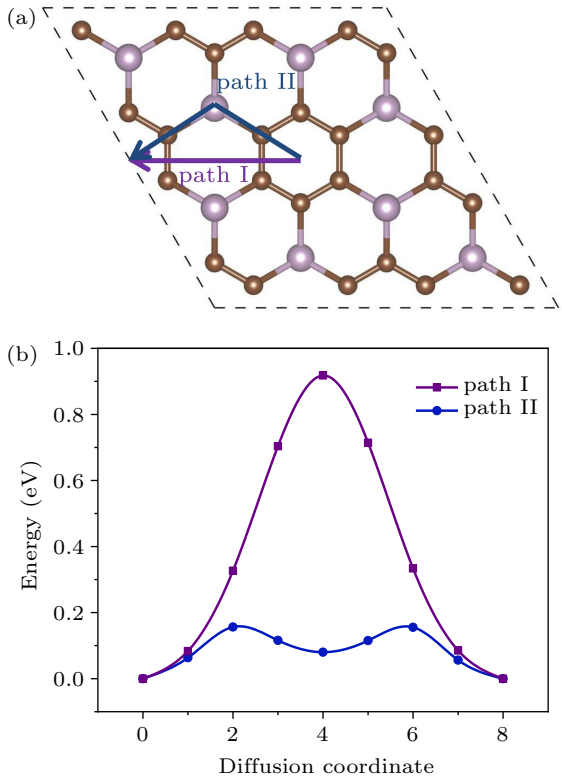


Fig. 3. (a) The diffusion paths and (b) corresponding diffusion energy barriers of K atom transfer on PC_3 surface.

3.3. Theoretical capacity and open-circuit voltage of PIBs with the anode of PC_3

The performance of ion batteries strongly depends on the storage capacity of metal atoms on anode materials, which is directly related to the number of adsorbed metal atoms on the substrate. To this end, K atoms can be absorbed layer by layer on both surfaces of the PC_3. The average adsorption energy of K atoms is obtained by

$$E_{\text{ave}} = (E_{n\text{K@PC}_3} - E_{\text{PC}_3} - nE_{\text{K}})/n, \tag{3}$$

where n is the total number of adsorbed K atoms, $E_{n\text{K@PC}_3}$ is the total energy of the K adsorbed PC_3, and E_{PC_3} is the energy of pristine PC_3. The negative adsorption energy indicates K atoms can be adsorbed stably.

Since K atoms have a tendency to form bulk spontaneously, we calculate the continuous adsorption energy of the additional layer E_{con} by the formula

$$E_{\text{con}} = E_{\text{K}_L/\text{PC}_3} - E_{\text{K}_{(L-1)}/\text{PC}_3} - 2\times 4\times E_{\text{K}}, \tag{4}$$

where L is the number of adsorbed layers, $E_{\text{K}_L/\text{PC}_3}$ and $E_{\text{K}_{(L-1)}/\text{PC}_3}$ are the total energy of L and $L-1$ layers K atoms adsorbed PC_3, respectively. So E_{con} should always be negative to make sure it is favorable of loading extra K layer on PC_3.

We load the first layer of K atoms at S1 on both sides of the substrate [see Fig. 4(a)]. After the optimization, all K atoms are steadily adsorbed. E_{ave} is calculated to be -0.50 eV,

and the vertical distance between K atoms and the sheet is 2.64 Å. Since S1 sites are fully occupied by the first K layer, there are two possible positions for depositing the second K layer (PC_3K_2), namely S5 and S6 sites. It turns out that K atoms prefer to occupy the S5 sites [see Fig. 4(b)]. With adsorbing two potassium layers on both sides of PC_3, E_{ave} decreases to −0.25 eV. The system remains energetically stable. To put the third K layer on, all the possible sites are considered, and S6 is the most favorable position; the optimized structure is shown in Fig. 4(c). The average adsorption energy is −0.19 eV. When connected with the cathode, a weak binding with anode is desired to enhance the voltage.[1] For the fourth K layer, the value of layer-by-layer average adsorption energy is positive, indicating that the adsorption becomes energetically unfavorable. For $L = 3$ to $L = 4$, E_{con} is −0.69 eV and 1.80 eV, respectively. Therefore, the limitation of loading K atoms is three layers on both sides, while the system maintains structural stability. The average adsorption energy ranges from −0.50 eV to −0.19 eV, which meets the requirement of ion batteries specifically.

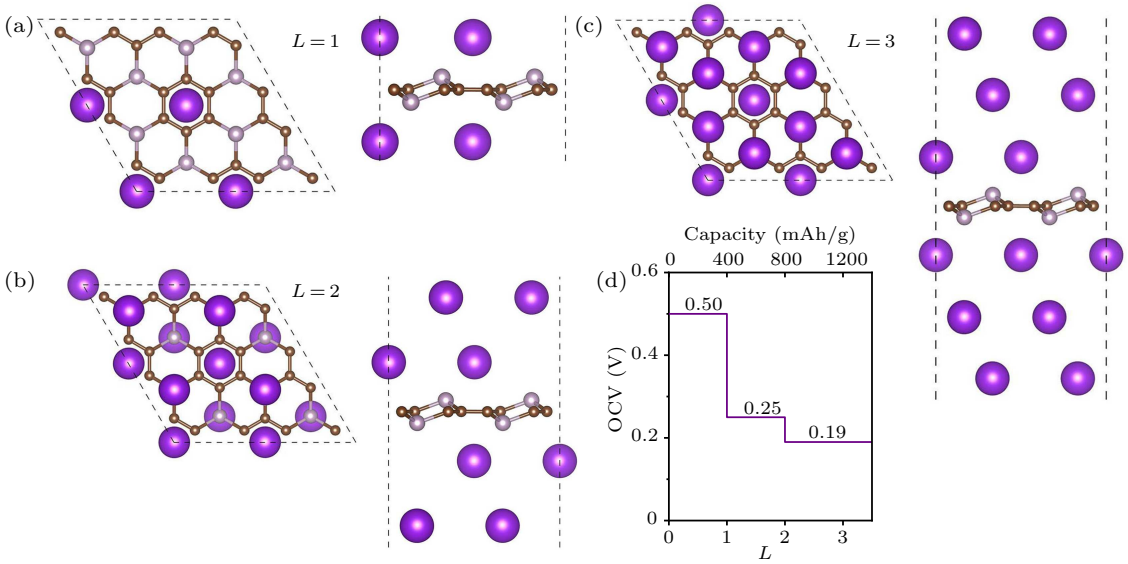


Fig. 4. Crystal structures of (a) PC_3K_1, (b) PC_3K_2, (c) PC_3K_3 from the side and top view. The violet balls indicate the K atoms. (d) Calculated OCV and theoretical capacity with different K adsorption concentrations.

Our electronic structural results show that, as the concentration of K atoms increases from one layer to three layers, the systems exhibit metallic characteristics and the subgaps below the Fermi level shrink. Correspondingly, the electronic conductivity of the PC_3 monolayer is enhanced with the increase of the concentration of K ions. The projected density of states (PDOS) is shown in Fig. 5; one can see the distinct overlap between the K-s orbital and the p orbitals of P and C at and around the Fermi level. Such significant s–p hybridization indicates notable interactions between potassium atoms and the PC_3 monolayer.

With the maximum K adsorption concentration on the PC_3, we evaluate its storage capacity using the following equation:

$$C = xF/M. \tag{5}$$

Here x is the number of electrons transferred, F is the Faraday constant, and M is the molecular mass of PC_3.[24] The storage capacity for the PC_3 monolayer is as large as 1200 mAh·g^{-1}, significantly larger than that of the black phosphorus anode for PIBs (617–843 mAh·g^{-1}),[25] and PC_6 in PIBs (781 mAh·g^{-1}).[26] Such a high storage capacity can be attributed to the variety of adsorption sites on both sides and the light atomic weight of P and C.

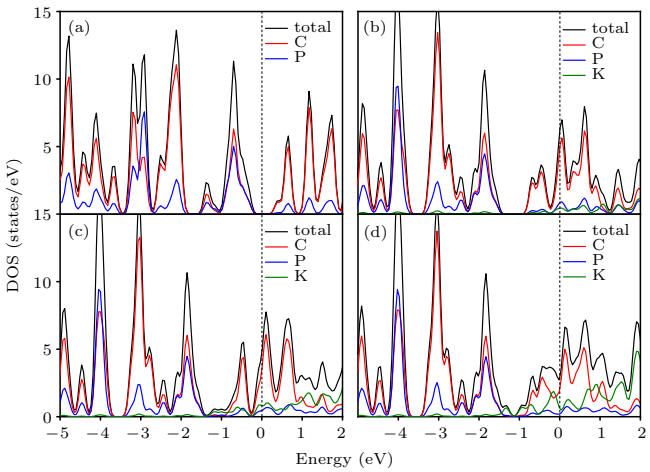


Fig. 5. Density of states for (a) PC_3, (b) PC_3K_1, (c) PC_3K_2, and (d) PC_3K_3. The Fermi level is set to 0 eV and labeled with vertical dashed lines.

Another significant parameter of ion batteries is open-circuit voltage (OCV), which can characterize the performance of anode materials for PIBs. The average open-circuit voltage can be calculated by

$$\mathrm{OCV} = (E_{\mathrm{K/PC_3}} - E_{\mathrm{PC_3}} - cE_{\mathrm{K}})/ce, \tag{6}$$

where c is the concentration of the adsorbed K atoms. The OCV decreases from 0.50 V, 0.25 V to 0.19 V with the increased number of adsorption layers. When the number of adsorbed K atoms reaches its limitation, we can obtain a fairly low OCV of 0.19 V. Such a low OCV can provide a large operating voltage with a higher energy density as applied in PIBs. Now we want to emphasize that the range of OCV is 0.19–0.50 V, which can avoid the formation of dendritic during the charge–discharge process.[27] This appropriate range of OCV values makes PC_3 an ideal candidate for anode material for PIBs.

4. Conclusion

By using first–principle calculations, we systematically investigate the structure stability and electronic property of the PC_3 monolayer, and find that the diffusion barrier of potassium on PC_3 is as low as 0.16 eV, ensuring the efficiency of the charging/discharging process. As an anode material, the PC_3 sheet has an ultra-high theoretical capacity of 1200 mAh·g^{-1}, which could guarantee the long-term durability of the battery. The value of OCV is between 0.19 V and 0.5 V, which can ensure the safety of the charging/discharging process. With low diffusion barrier, high capacity, and suitable OCV, we predict that PC_3 is an ideal choice for PIBs anode materials.

References

[1] Liu Y Y, Merinov B V and Goddard W A 2016 *Proc. Natl. Acad. Sci. USA* **113** 3735

[2] Bie X F, Kubota K, Hosaka T, Chihara K and Komaba S 2017 *J. Mater. Chem. A* **5** 4325

[3] Yoo E J, Kim J, Hosono E, Zhou H S, Kudo T and Honma I 2008 *Nano Lett.* **8** 2277

[4] Mayo M, Griffith K J, Pickard C J and Morris A J 2016 *Chem. Mater.* **28** 2011

[5] Guo G C, Wang D, Wei X L, Zhang Q, Liu H, Lau W M and Liu L M 2015 *J. Phys. Chem. Lett.* **6** 5002

[6] Wang T, Guo W, Wang G, Wang H, Bai J and Wang B B 2020 *J. Alloy. Compd.* **834** 155265

[7] Sannyal A, Zhang Z Q, Gao X and Jang J 2018 *Comp. Mater. Sci.* **154** 204

[8] Gong S, Zhang C, Wang S and Wang Q 2017 *J. Phys. Chem. C* **121** 10258

[9] Shen Y P, Liu J, Li X Y and Wang Q 2019 *ACS. Appl. Mater. Inter.* **11** 35661

[10] Zhao Z Y, Yu T, Zhang S T, Xu H Y, Yang G C and Liu Y C 2019 *J. Mater. Chem. A* **7** 405

[11] Jana S, Thomasb S, Lee C H, Jun B and Lee S U 2019 *Carbon* **157** 420

[12] Dou K Y, Ma Y D, Zhang T, Huang B B and Dai Y 2019 *Phys. Chem. Chem. Phys.* **21** 26212

[13] Lv X S, Wei W, Huang B B and Dai Y 2019 *J. Mater. Chem A.* **7** 2165

[14] Kresse G and Furthmuller J 1996 *Phys. Rev. B* **54** 11169

[15] Kohn W and Sham L J 1965 *Phys. Rev.* **140** A1133

[16] Perdew J P, Burke K and Ernzerhof M 1996 *Phys. Rev. Lett.* **77** 3865

[17] Monkhorst H J and Pack J D 1976 *Phys. Rev. B* **13** 5188

[18] Blöchl P E 1994 *Phys. Rev. B* **50** 17953

[19] Grimme S, Antony J, Ehrlich S and Krieg H 2010 *J. Chem. Phys.* **132** 154104

[20] Ganguly R and Jevtovic V 2017 *Acta. Crystallogr.* **73** Pt 8

[21] Becke A D and Edgecombe K E 1990 *J. Chem. Phys.* **92** 5397

[22] Zhou L J, Hou Z F and Wu L M 2012 *J. Phys. Chem. C* **116** 21780

[23] Kuzubov A A, Eliseeva N S, Krasnov P O, Tomilin F N, Fedorov A S and Lykhin A O 2012 *J. Exp. Theor. Phys.* **114** 1018

[24] Zhang T, Ma Y D, Huang B B and Dai Y 2019 *ACS Appl. Mater. Inter.* **11** 6104

[25] Sultana I, Rahman M M, Ramireddy T, Chen Y and Glushenkov A M 2017 *J. Mater. Chem. A* **5** 23506

[26] Yang E, Ji H, Kim J, Kim H and Jung Y 2015 *Phys. Chem. Chem. Phys.* **17** 5000

[27] Eames C and Islam M S 2014 *J. Am. Chem. Soc.* **136** 16270